AJNR

MR Imaging Anatomy in Neurodegeneration: A Robust Volumetric Parcellation Method of the Frontal Lobe Gyri with Quantitative Validation in Patients with Dementia

B. Iordanova, D. Rosenbaum, D. Norman, M. Weiner and C. Studholme

AJNR Am J Neuroradiol 2006, 27 (8) 1747-1754
http://www.ajnr.org/content/27/8/1747

ORIGINAL RESEARCH

MR Imaging Anatomy in Neurodegeneration: A Robust Volumetric Parcellation Method of the Frontal Lobe Gyri with Quantitative Validation in Patients with Dementia

B. Iordanova
D. Rosenbaum
D. Norman
M. Weiner
C. Studholme

BACKGROUND AND PURPOSE: Brain volumetry is widely used for evaluating tissue degeneration; however, the parcellation methods are rarely validated and use arbitrary planes to mark boundaries of brain regions. The goal of this study was to develop, validate, and apply an MR imaging tracing method for the parcellation of 3 major gyri of the frontal lobe, which uses only local landmarks intrinsic to the structures of interest, without the need for global reorientation or the use of dividing planes or lines.

METHODS: Studies were performed on 25 subjects—healthy controls and subjects diagnosed with Lewy body dementia and Alzheimer disease—with significant variation in the underlying gyral anatomy and state of atrophy. The protocol was evaluated by using multiple observers tracing scans of subjects diagnosed with neurodegenerative disease and those aging normally, and the results were compared by spatial overlap agreement. To confirm the results, observers marked the same locations in different brains. We illustrated the variabilities of the key boundaries that pose the greatest challenge to defining consistent parcellations across subjects.

RESULTS: The resulting gyral volumes were evaluated, and their consistency across raters was used as an additional assessment of the validity of our marking method. The agreement on a scale of 0–1 was found to be 0.83 spatial and 0.90 volumetric for the same rater and 0.85 spatial and 0.90 volumetric for 2 different raters. The results revealed that the protocol remained consistent across different neurodegenerative conditions.

CONCLUSION: Our method provides a simple and reliable way for the volumetric evaluation of frontal lobe neurodegeneration and can be used as a resource for larger comparative studies as well as a validation procedure of automated algorithms.

MR imaging is emerging as a central tool for in vivo quantification of human brain anatomy in studies of both disease and normal aging. High-resolution MR imaging allows detailed characterization of the major cortical structures.[1] One of the key areas of interest is the study of neurodegenerative conditions, in which volumetric changes in local or global anatomy may provide a more accurate and reproducible indication of disease state and progression than conventional clinical diagnostic criteria.[2] Regional brain tissue volumes are often used as the basic physical measure of in vivo brain anatomy, to which functional change may be related both during normal aging and in the presence of pathology.[3]

The key motivation for this project was to provide a reference standard for the evaluation and improvement of automated morphometric tools to quantify atrophy patterns. A wide range of automated and semiautomated morphometric tools have been proposed in the literature,[4] and the results of some are widely reported, stating relationships between regional tissue volume loss and overall clinical diagnosis or change in functional performance.[5] Overall, it is rare that automated morphometric methods are published with a quantitative evaluation of their cross-sectional accuracy in the type of data to which they are being applied. Studies that make some effort in the validation direction often do not provide details of the image processing procedure and a description of the specific boundaries they used to obtain the volumes.[6] Attention is paid to correlating gyral volumes, but no evaluation of the accuracy of the location of the markings[7] is provided.

The starting point for the evaluation of tissue loss in neurodegeneration is a commonly accepted definition of corresponding local anatomy in different subjects. However, in comparing anatomic measures between subjects, significant variations in brain structure, especially in gyral pattern, present innate challenges to quantitative brain analysis. A second major inherent difficulty in clinical studies of neurodegenerative disease is the accurate description of anatomic subregions, whose definitions are themselves robust to the disease process being studied. Examination of many published protocols for brain parcellation reveals the possibility for such a change in procedure to occur: specifically, where subregions (eg, the frontal pole or temporal pole) are defined by using landmarks that are significantly external to the region being studied. A classic example is the use and dependence of marking protocols on "standardized orientation," and the application of orthogonal planes based on axes derived from such a standardized reorientation procedure. In such cases, bulk loss of tissue (for example in the frontal or parietal white matter) may significantly modify the relationship between cortical structures and the deeper internal landmarks and coordinate systems based on them (such as the anterior commissure-posterior commissure line). Any cortical parcellation that relies

Received June 10, 2005; accepted after revision December 16.

From the Department of Radiology, Magnetic Resonance Unit, San Francisco Veterans Affairs Medical Center and the University of California, San Francisco, Calif.

This work was funded by a Whitaker foundation award RG-01-0115 and NIH grants R01 MH65392 and RO1 EB00822. The imaging and clinical data were acquired as part of NIH grants P01 AG12435, NIA P01 AG19724, PO1 AA11493, and R01 AG10897.

Please address correspondence to: Bistra Iordanova, PhD, 601 Mellon Institute, Carnegie Mellon University, 4400 Fifth Av, Pittsburgh, PA 15213; e-mail: biordano@andrew.cmu.edu

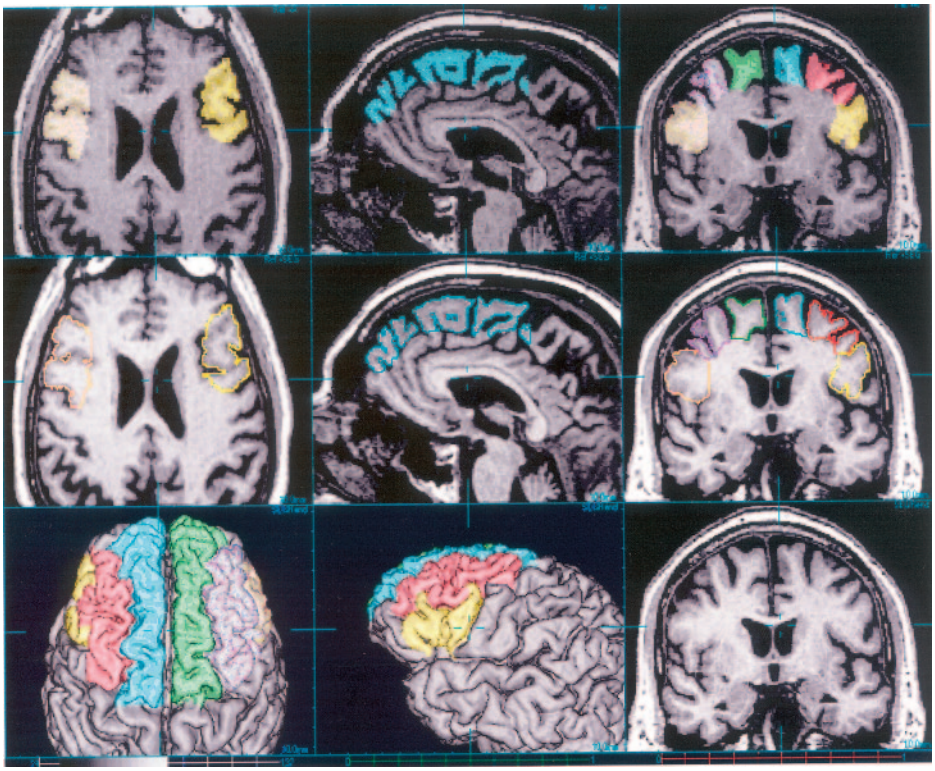

Fig 1. A screen capture showing the general layout of the tracing software used, with overlay, outline, and surface views. The user can scroll through planes along any of the 3 main axes, use crosshairs for precise multiplanar viewing, zoom in and out, and rotate the view. The surface-rendering can be aligned or oriented independently to the section displays, and a common reference point at the crosshairs can be maintained.

on a consistent relationship between features spatially remote from the regions being studied cannot be expected to report quantitatively meaningful volumes for cortical subregions. Ideally, the regional definitions used must, as much as possible, be intrinsic to the structures being studied.

The frontal lobe consists of a significant proportion of the human cortex, and the effect of neurodegeneration on its structure and function often involves an examination of the effects on focal subregions. Although many fine-scale definitions of functional areas, such as those of Brodmann,[8] are possible, in practice to study anatomy via clinical MR imaging, definitions realistically have to be limited to those features consistently visible and definable in the image data acquired. The purpose of the present study was to create an explicit frontal lobe parcellation method that is robust to varying states of neurodegeneration and individual variability and that is easy for others to reproduce. It is based on a commonly used high-resolution magnetization-prepared rapid acquisition of gradient echo (MPRAGE) structural imaging protocol that provides good balance between tissue contrast, resolution, and geometric integrity, though the general approach is applicable to any 3D sequence with comparable or better isotropic spatial resolution.

Materials and Methods

Subjects and Imaging Data

To develop and evaluate the tracing procedure, we used MR imaging scans from a total of 25 subjects whose structural MR imaging data were selected from a group of patients studied in research projects of dementia and aging at the San Francisco Veterans Hospital and the University of California, San Francisco Memory and Aging Center. The subjects had different levels of cortical tissue degeneration, ranging from normal for the age to severe. All subjects provided informed consent before participation. We looked at 3 major population groups: healthy controls (9 subjects, 4 women and 5 men with a mean age 62 $\pm$ 8), 8 subjects with Lewy body dementia (LBD) (2 women and 6 men with a mean age of 74.6 $\pm$ 9.2), and 8 subjects with Alzheimer disease (AD) (3 women and 5 men with a mean age of 78 $\pm$ 5.7). The AD diagnoses were made according to the criteria of the National Institute of Neurologic and Communicative Disorders and Stroke-Alzheimer Disease and Related Disorders Association. The data used for the current parcellation protocol consisted of T1-weighted coronal images obtained on a Siemens 1.5T MR imaging system by using an MPRAGE sequence (TR/TE/TI, 10/4/300 ms; flip angle, 15°; 6/8 field of view, 256 $\times$ 256 mm^2 with 1.0 $\times$ 1.0 mm^2 in-plane resolution; 164 partitions with 1.5 mm thickness).

Image Visualization and Tracing Tool

The imaging data were prepared for manual delineation by using a semi-interactive manual tracing tool, which allows outlining of brain regions based on manually defined contrast and geometry, by using refinements of the freely distributed Rview medical registration and display software (http://rview.colin-studholme.net). The software allows fast semiautomated definition of the brain surface for cortical visualization while tracing. The surface-rendering was used only for visualization, and the entire tracing was carried out on multiple orthogonal planes.

Delineation was performed with a semiautomated tracing method on MR imaging planes displayed in an interactively updated display, incorporating simultaneous axial, coronal, and sagittal section views

(Fig 1). MR imaging contrast and brightness can be directly controlled by interactively varying the mapping between MR imaging values and a user-selected gray-scale to allow the tracer to optimally view different tissue boundaries. Voxels to be labeled with a given definition are assigned a number and an associated color, displayed either as a color wash overlaid on the gray-level MR imaging or as a set of color-coded contours signifying region boundaries on the MR imaging intensities. The label applied by the tracing could be modified as the tracing proceeded, to adjust boundaries between neighboring regions. The semiautomated tracing procedure is designed to permit high-contrast boundaries to be automatically delineated, while the parts of the contour requiring user-dependent definition are determined by the movement of the mouse or another 2D input device. This result was achieved by the tracing being limited to a manually adjustable range of MR imaging intensities, allowing, for example, region delineation to be constrained to a given high-contrast tissue or set of tissues. As a result, in our tracing procedure, the user generally chose to constrain tracing to higher intensity values corresponding to gray or white matter and excluding all tracing from darker regions corresponding to CSF. Thus, the outer CSF-tissue boundary was determined by the tracing intensity range selected by the user, whereas the within-tissue region boundaries were directly dependent on the user tracing. All tracings were completed by using a standard 2-button mouse and a PC-based 32-bit display, allowing 256 different pure-gray levels and a total of 2^{24} different colors. The relative orientations of the displayed planes cutting through the data can also be interactively modified to create oblique plane views at any angle and around any point of the MR imaging anatomy.

Manual tracing was performed with simultaneous multiplanar assessment of the current labeled region (ie, if a region of interest was labeled in the axial view, the region could be observed in the other 2 orientations and thus corrected if it deviated from the intended borders). Multiplane views could display regions either with a color wash overlay or as a set of contours: The contour display generally permits a clearer evaluation of the tissue contrasts within and between traced regions, whereas a solid color wash allows continuity of a complex structure cutting through a plane to be appreciated. In addition, other types of views are available, including combinations of surface-rendered and section views, all updated with label colors as tracing proceeds. The coloring of cortical surfaces with underlying labels permits the direct evaluation of the progression of tracing with respect to the cortical folds. Cut planes can also be used in the surface-rendered views to explore the depth of tracing with respect to the cortical surface. Views with different zooms combined in 1 display allow the user to track the global context of the fine-scale tracing being done on a local region of the brain. On average, it took 3–4 hours for the preprocessing and manual parcellation of the specified regions.

Manual Tracing Protocol

Because of the fine-scale complexity of their boundary, gray and white matter are generally separated by using automated tissue-segmentation techniques.[9] Here, we, therefore, have focused on the basic definition of gyral tissue as a combination of gray and white matter structures between and above the basins of adjacent sulci. The border we used to delineate the internal extent of the gyral region used a line connecting the deepest points of the adjacent sulci.[7,8] Several major sulci with relatively high rates of continuity were designated as region landmarks to determine the extent of the definitions along gyral folds.[10]

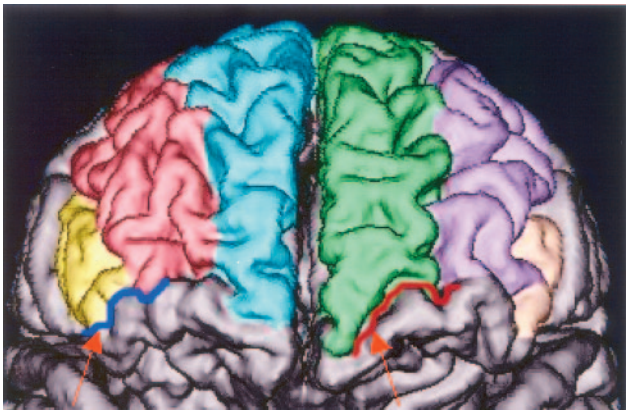

Fig 2. A view of the frontal pole showing the frontal marginal sulcus (*right arrow, red line*) and lateral orbital sulcus (*left arrow, blue line*) used as borders between the lateral and the ventral part of the frontal lobe. The SFG is in blue on the left and in green on the right.

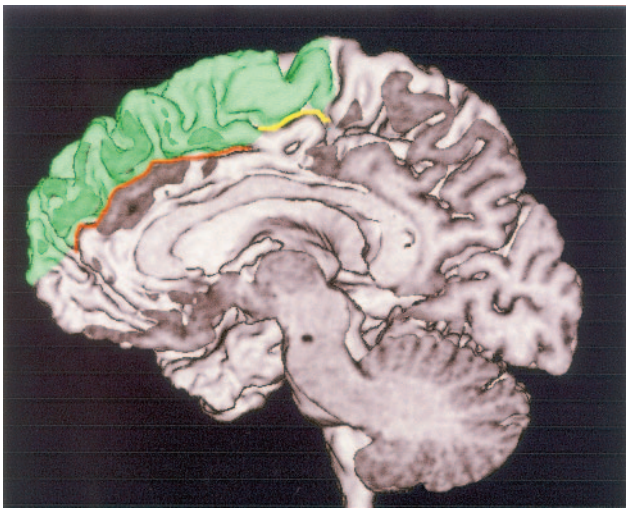

Fig 3. A medial view of the SFG (in green) showing an interruption of the cingulate sulcus, for which we defined the border as a straight line connecting the anterior (brown) and posterior (yellow) parts.

Superior Frontal Gyrus

Boundaries. We defined the superior frontal gyrus (SFG) as the most superior gyrus in the frontal lobe. Its medial border is the interhemispheric fissure, and its lateral border is the superior frontal sulcus (SFC). The key borders most difficult to define are those determining the posterior and anterior extent, together with the border with the cingulate gyrus. We will describe each of these in detail.

Anterior Extent. Anteriorly, the SFG extends to the frontal marginal sulcus (FMS). Using the FMS as the anterior border necessitates inclusion of the transverse frontopolar gyri into the superior and middle frontal region. The reasoning behind this inclusion is the large anatomic variation of frontopolar area between subjects. Consequentially, there is no plausible definition of the transverse frontopolar gyri that can be applied in a consistent manner and be reproduced in different subjects.[11] The FMS is a reliable sulcus with high rates of continuity,[10] and we used it as a border between the lateral and ventral part of the frontal lobe (Fig 2).

Inferior Extent. The most prominent sulcus on the medial surface is the cingulate sulcus (CingS), which we used as the inferior border of SFG. In cases of CingS interruption, we used a straight line that connects its anterior and posterior parts (Fig 3). The highly variable presence of the paracingulate sulcus (PCingS) superior to the CingS pre-

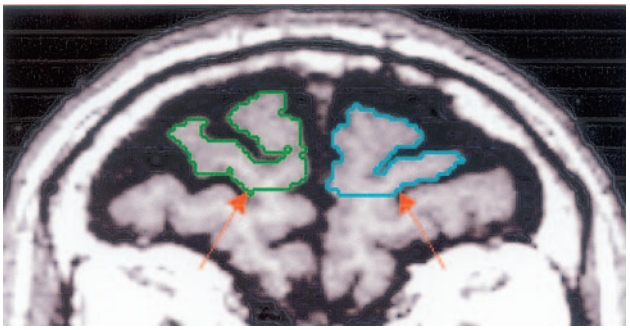

Fig 4. The frontal marginal sulcus defining the anterior border of the SFG is easily identifiable on anterior coronal sections (*arrows*, indicating this sulcus on the left and right hemisphere).

sents a real challenge for strict gyral definition.[12,13] According to volumetric studies, the PCingS is more common on the left side of men, and it is inversely correlated with the volume of the cingulate gyrus.[14] However, there are no data to date that correlate the volume of the SFG with the size and sulcal pattern of the neighboring cingulate region. For the purposes of the SFG definition, when a PCingS was present in a complete uninterrupted form, we used it as an inferior border of the SFG. When the PCingS was present in an interrupted form, we connected its anterior and posterior branches and used that line as the inferior border of the SFG.

Posterior Extent. The precentral sulcus (PreCS) runs perpendicular to the 3 major frontal gyri, and it is easily identified as the SFG posterior border on axial and sagittal sections. Some parcellation schemes[7] define the paracentral lobule as a separate structure between the SFG and the precentral gyrus (PreCG); however, in our protocol, it is included in the caudal SFG region. The reasoning behind this inclusion is that the definition of the lobule requires the presence of the paracentral sulcus (PCentrS), which is very often absent from the medial wall of the brain or has a great variation in patterns.[10]

Procedure. Initially the FMS was identified on the most anterior coronal sections, and those markings defined how far the frontal gyri extended anteriorly. The FMS is the border between the SFG and the frontomarginal gyrus. The FMS is the first sulcus that separates the ventral from the orbital portion at the area of the frontal pole (Fig 4). The tracing continued on the most superior axial sections moving inferiorly as long as the SFC could be identified as a distinguishable border between the SFG and middle frontal gyrus (MFG). In cases where the SFG occasionally ramified and had 2 branches running parallel, they were both included by following their natural pattern (Fig 5).

Inferior Frontal Gyrus

The inferior frontal gyrus (IFG) was traced after completion of the SFG, leaving the cortical area between the SFG and IFG to constitute the MFG region.

Boundaries. The inferior frontal sulcus (IFS) separates the IFG from the MFG. It constitutes the superior border of the IFG and the inferior border of the MFG, and its continuity rate is relatively good.[10] In cases of interruption, we connected the deepest points of the segments of the IFS with a straight line that optimally follows their course (Fig 6).

The inferior part of the PreCS bounds the IFG caudally. Posteriorly, the IFG is bounded by the circular sulcus of the insular and the Sylvian (lateral) fissure. The 2 rami of the Sylvian fissure, horizontal and vertical, define the 3 parts of the IFG: the pars orbitalis rostrally, the pars triangularis centrally, and the pars opercularis caudally.[15,16] Anteriorly, where the FMS disappears along the frontal part of the frontomarginal gyrus,

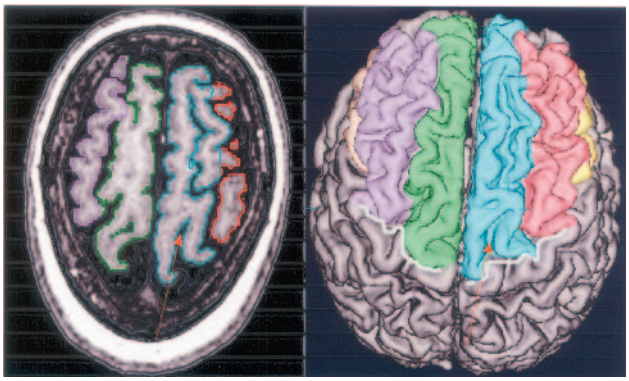

Fig 5. The SFG on the right hemisphere of this subject ramifies into 2 branches (left panel), and we defined the region of the gyrus to include both branches, taking into account its natural pattern. The point of ramification is indicated by the arrow. The surface-rendering on the right panel shows the posterior border of this gyrus—the PreCS marked with a white line.

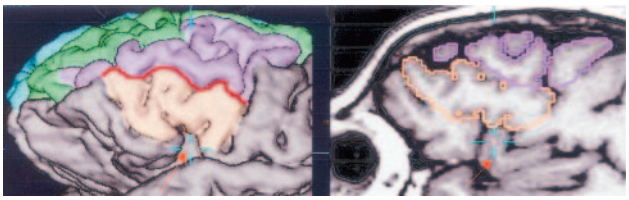

Fig 6. The IFS is marked here with a red line on the surface-rendering. It separates the IFG (brown) from the MFG (purple), and in cases of its interruption, we connected the separate pieces to form a continuous line. The arrow shows the insula and the relative position of the IFG and the insula. The sagittal plane is most useful for distinguishing the border between these 2 structures.

the lateral orbital sulcus (Fig 2) was used to inscribe the rostral and the inferior borders of the IFG and the insula.[9,17]

Procedure. The IFG was initially marked on the lateral sagittal sections, scrolling toward the midline. The 3 parts of the IFGs described previously are easily identifiable on this orientation. Sagittal images can also be used as well to verify the relative position of IFG and the insula (Fig 6). In cases where the PreCS did not separate the PreCG from the IFG completely, a straight line was drawn from the fundus of PreCS to the Sylvian fissure to inscribe the posterior border.

Middle Frontal Gyrus

Boundaries. The SFC is the superior border of MFG, and the IFG is its inferior border. Posteriorly, the MFG extends to the PreCS, and where the PreCS has superior and inferior parts, the line that connects those 2 parts constitute the posterior border of MFG (Fig 7).

Anteriorly, the MFG extends to the FMS and includes part of the transverse frontopolar gyri. The latter stream out of MFG and represent its natural continuation at the frontal polar area. The MFG usually has 2 parts, superior and inferior, that are separated by the middle frontal sulcus. In those cases, both branches were included in the region of interest.[15]

Procedure. The MFG is marked on a coronal orientation as the gyrus between the SFG and the IFG and, sagittally, on the sections where it first appears above the IFG. It can be traced as well on superior axial images where is appears proximal to the SFG.

Tracing Data Analysis

The parcellation of 3 major gyri of 25 subjects provided us with raw volume data of those structures; mean and standard deviations of those volumes were computed and are presented in the Results sec-

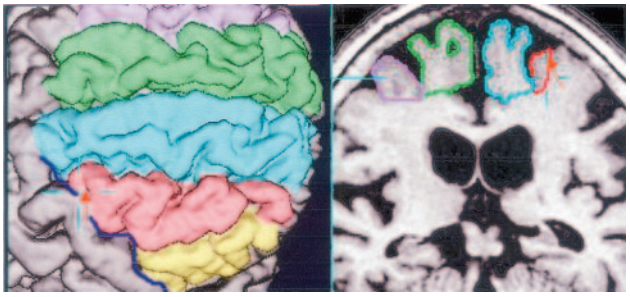

Fig 7. The PreCS (shown with a *blue line* on the left panel) defines the posterior border of the MFG (in red). The left panel shows an example of this sulcus segmented into 2 pieces; the arrow indicates the exact location of the interruption. In such cases, we connected the segments with a line following the natural course of the sulcus.

tion. We evaluated the reliability and reproducibility of the parcellation protocol by re-marking 6 randomly chosen subjects of the total 25 subjects in the study. The rater who marked the 25 subjects re-marked the 6 randomly chosen subjects after 8 months, blinded to the initial parcellation and to the diagnosis. An additional outside rater was given the same 6 datasets and marked the same areas following our parcellation protocol, blinded to diagnosis and the markings of the first rater. The resulting parcellations contained a total of 102 gyral markings—6 subjects each had 6 gyri marked 3 separate times. These segmentations were stored in the form of image data, in which each voxel location holds a label value. The diagnoses of the 6 randomly chosen subjects to which the raters were blinded were the following: healthy control (3 subjects), LBD (2 subjects), and AD (1 subject). The level of tissue degeneration varied widely in the dataset; this feature brought additional importance to the consistency of our method.

The 2 types of information, gyral volumes and gyral spatial boundaries, were evaluated quantitively by using a volume similarity coefficient (VSC) and a spatial overlap coefficient (SOC). We computed volume similarity coefficients between the volumes obtained from the 2 different raters and between the 2 time points of the same rater by using the formula[18]:

$$\mathrm{VSC} = 1 - \frac{|\text{Volume first rating} - \text{Volume second rating}|}{\text{Mean of the two volumes}}$$

The VSC was averaged over the 102 gyral markings of the 6 randomly chosen subjects by the 2 raters. Thus, the closer VSC value was to 1, the more similar were the 2 estimated volumes. The absolute value of the difference between the 2 parcellations reflects equally any under- or overestimates. By normalizing by the mean volume, we assume that the true gyral volume is closest to the average of all parcellations.

The VSC can only tell us how similar the volumes were; it cannot tell us if the different markings actually defined the same locations in the 2 anatomies. This difference is important because 2 observers may consistently use slightly different definitions of anatomy that are highly related in volume but are not the same anatomic structure. Distinguishing this possibility is important because a disease may then modify this relationship so that the 2 slightly different anatomic definitions that had closely related volumes may then not be related in volume (eg, only 1 of the definitions includes the subregion influenced by disease). To examine the consistency of the 2 definitions, we computed the SOC from the intersection as follows[19]:

$$\mathrm{SOC} = \frac{\text{No. of voxels at intersection of 2 different markings}}{\text{Mean of the voxels of the 2 parcellations}}$$

Table 1: Volume similarity and spatial overlap coefficients for the same rater

Segmented Structures for 6 Subjects	Mean Volume Similarity Coefficient	Mean Spatial Overlap Coefficient
SFG (right)	0.92 ± 0.12	0.85 ± 0.03
SFG (left)	0.90 ± 0.11	0.85 ± 0.05
MFG (right)	0.94 ± 0.05	0.84 ± 0.03
MFG (left)	0.92 ± 0.03	0.84 ± 0.01
IFG (right)	0.84 ± 0.14	0.83 ± 0.04
IFG (left)	0.89 ± 0.09	0.81 ± 0.08
Overall	0.90 ± 0.10	0.84 ± 0.05

Note:—SFG indicates superior frontal gyrus; MFG, middle frontal gyrus; IFG, inferior frontal gyrus.

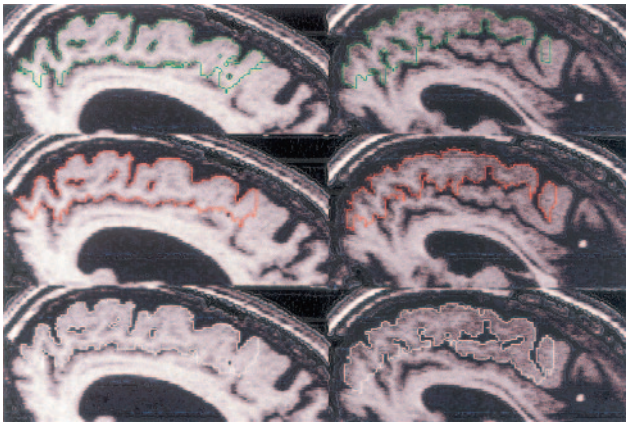

Fig 8. SOCs computed for the same rater who marked 5 subjects twice show the intra-rater variability for each individual scan and region. Bars are grouped by left and right brain region, and subjects are color-coded.

Means of the spatial overlap between the markings of the 2 raters and between the 2 time points of the same rater were computed and are presented in the Results section.

To numerically evaluate this, we randomly picked a subject's scan out of the AD group (8 subjects) originally marked by a single rater. This dataset was then re-oriented (with respect to the 3 rotations and 3 translations governing patient orientation) by an independent observer, to simulate differences in patient positioning within the scanner. The manually selected transformations were applied by using a 5-point sinc interpolation to re-sample the voxels into a new voxel grid. A rater, blinded to the exact nature of the new orientation or previous parcellations, followed the same procedure and re-marked the new dataset. We compared the volumes of the obtained structures by computing the VSC.

Results

Intra-Rater Evaluation

One rater traced a subset of 6 of the 25 scans twice, separated by an 8-month interval. Table 1 reports the volume similarity and spatial overlap coefficients for the 2 time points of the same rater. Figure 8 shows the intra-rater variability for each individual scan and region. The average spatial overlap of the repeated markings of the same rater was 0.84 ± 0.05 on a scale of 0–1, where zero is equivalent to no overlap and 1 indicates full overlap of the 2 segmentations. The mean volume agreement was 0.90 ± 0.10 on a scale of 0–1, where the disagreement of 0.1 corresponds on average to 2.1 cm^3 of marked tissue. The horizontal axis of Table 1 shows the marked re-

Table 2: Volume similarity and spatial overlap coefficients between 2 raters

Segmented Structure	Volume Similarity Coefficient	Spatial Overlap Coefficient
SFG (right)	0.93 ± 0.12	0.87 ± 0.05
SFG (left)	0.91 ± 0.15	0.88 ± 0.04
MFG (right)	0.97 ± 0.02	0.84 ± 0.09
MFG (left)	0.88 ± 0.13	0.87 ± 0.04
IFG (right)	0.85 ± 0.14	0.85 ± 0.02
IFG (left)	0.91 ± 0.10	0.81 ± 0.04
Overall	0.91 ± 0.11	0.85 ± 0.06

Note:—SFG indicates superior frontal gyrus; MFG, middle frontal gyrus; IFG, inferior frontal gyrus.

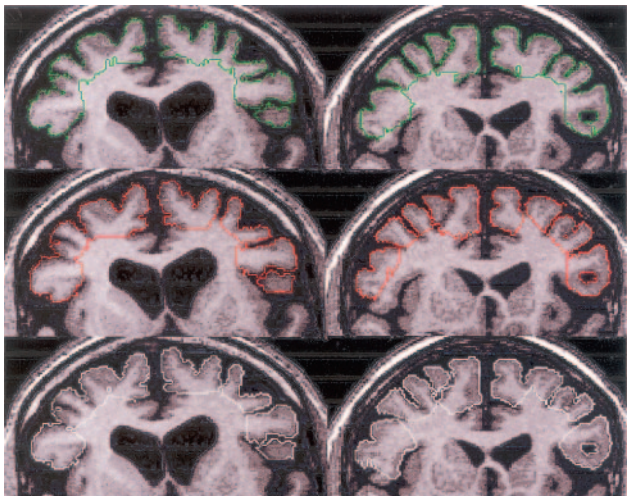

Fig 9. SOCs for the 2 different raters show the spatial overlap across all 5 subjects, averaged for the marked regions left and right. The different subjects are color-coded.

gions, and the vertical axis shows the value of the SOC. These confirm that the tracer was consistently marking between 80% and 90% of the region identically for most subjects. Subject D was the least consistently traced, with appreciably lower agreement in the SFG-left and the IFG-left.

Inter-Rater Evaluation

For the between-rater comparisons on 6 randomly chosen subjects, the VSC and SOC are presented in Table 2. These were computed according to the formulae given in the previous section to measure the inter-rater variability for each of the regions of interest that we studied. The average spatial overlap between the 2 raters was 0.85 ± 0.06, where again zero indicates no overlap and 1 is equivalent to full spatial overlap. The mean volume agreement was 0.91 ± 0.11 on a scale of 0–1, where the volume disagreement between the 2 raters corresponds on an average of 1.8 cm^3. Coefficient values close to 1 show a good agreement in each of the 6 gyral regions, with the lowest overall agreement occurring in the right IFG.

Fig 9 represents graphically the spatial overlap coefficients across all 5 subjects averaged for marked region left (frontal gyrus left) and right (frontal gyrus right). The different subjects are color-coded. Overall the agreement between observers was comparable to that within the observer, with 1 or 2 subjects showing lower agreement.

Independence of Head Position and Angulation

One dataset was chosen at random and transformed into a different head position and angulation. The new head position in space was significantly altered by re-slicing the data with respect to all 3 axes, thus revealing completely different cross-sectional shapes than the ones first marked. One of the raters re-marked the same regions of interest blinded to the exact repositioning and previous parcellations of the same subject. The volumetric agreement of the new orientation data with the data from the original orientation was found to be 0.96. This number is the mean value of the 6 brain regions per dataset. Such high agreement between region volumes, despite the fact that they were marked in a completely different head orientation, shows that protocol is independent of head position. The diagnosis of the subject was AD with relatively severe tissue atrophy.

Raw Volumes

The mean raw volumes (in cubic centimeters) of the delineated regions of all subjects in the 3 groups are summarized in Table 3, together with their standard deviations. The values are separated according to the 3 different groups: controls, AD, and LBD.

Specific Examples of the Sources of Marking Variability

Following numeric evaluation of the results, we visually inspected the tracing marks of the 2 raters to investigate the main source of differences in the final anatomic markings. This revealed 3 main areas of difference:

The Superior Frontal Gyrus Depth of Marking. Although the gyral depth was defined as the line between the fundus of 2 neighboring sulci, in the presence of the partial PCingS, the inferior border of the SFG was difficult to define. Figure 10 demonstrates good spatial overlap in column 1 and bad spatial overlap between the rows 2 and 3 on the second column.

Posterior Inferior Frontal Gyrus. Because the paracentral sulcus (PCentrS) is frequently discontinuous at the level of pars opercularis, the marking in the coronal orientation can extend an additional few sections posteriorly (Fig 11). To avoid this problem, we recommend using the sagittal view to note the course of the PCentrS.

Double Frontal Marginal Sulcus. In the rare cases of a double FMS, the most superior branch has to be chosen to achieve reproducibility across subjects.

Discussion

In this article, we presented and quantitatively evaluated a parcellation method for the delineation of the 3 major frontal lobe

Table 3: Average values of gyral tissue volume (cc, bilateral) for all patients bilaterally

Patients	SFG (Right)	SFG (Left)	MFG (Right)	MFG (Left)	IFG (Right)	IFG (Left)
Controls (n = 9)	35.3 ± 4.2	33.6 ± 5.5	23.8 ± 2.9	25.3 ± 2.1	13.4 ± 1.8	13.2 ± 1.7
Alzheimer disease (n = 8)	33.0 ± 3.9	30.3 ± 3.4	20.2 ± 3.2	20.3 ± 2.5	10.9 ± 2.7	10.9 ± 1.6
Lewy body dementia (n = 8)	31.8 ± 5.2	29.9 ± 4.3	19.7 ± 3.1	20.2 ± 3.1	12.2 ± 2.6	11.2 ± 2.2

Note:—SFG indicates superior frontal gyrus; MFG, middle frontal gyrus; IFG, inferior frontal gyrus.

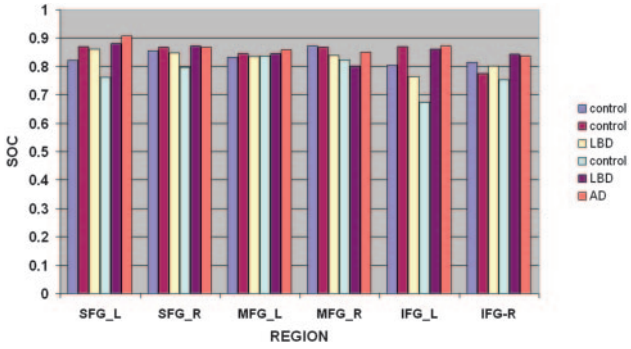

Fig 10. A comparison of the markings of the SFG by the same rater (rows 1 and 2) and the second rater (row 3). The first column shows high rater agreement. The second column (last panel) shows a relative overestimation of the inferior extent of the SFG.

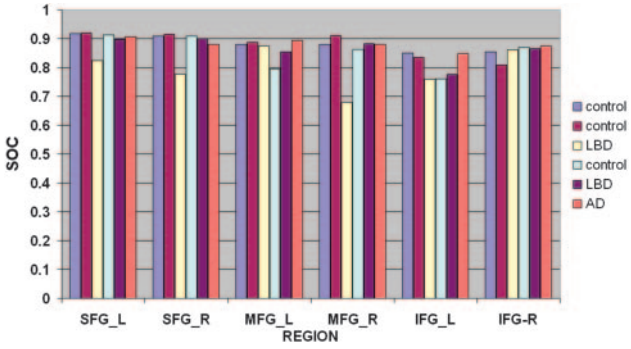

Fig 11. Results on 2 subjects (left and right). The segmentation of the subject in the first column shows good spatial overlap between raters. The tracing on the subject in the second column shows significant variability in the definition of the depth of the left IFG.

regions from conventional high-resolution T1-weighted structural MR imaging, specifically aimed at the study of neurodegenerative disease. By limiting our anatomic definitions to landmarks intrinsic to those regions being delineated and avoiding the use of externally defined dividing planes, we ensured that changes in the surrounding anatomy, such as modifications in the relationship between the anterior commissure-posterior commissure line and the cerebral cortex, do not confound the local gyral definitions.

Although many methods for parcellation have been described in the literature, none have been aimed at the specific problem of volumetry in neurodegeneration, and most important, none have reported the error in marking the same voxels with a given anatomic label by different observers (overlap). Validation is often limited entirely to differences in the summary volume delineated, not to where that volume was placed in the underlying anatomy. The 2 main previous articles to report any evaluation of the tracing results from more than 1 observer in similar anatomic regions are those of Tisserand et al[20] and Kennedy et al.[11] Tisserand et al reported intraclass correlation coefficients of frontal cortical tissue volume (not overlap) in manually selected cubic subvolumes of 5 subjects. They reported agreement in volumes by different observers (IFG left and right, 0.98 and 0.94), (grouped SFG and MFG together left and right, 0.97 and 0.96), but only after identical steps of stereotaxic alignment were first applied for each observer. The anatomic border definitions themselves relied heavily on 4 externally defined slicing planes mutually parallel to each other in the reformatted anatomy.

The other study[11] also relied on borders containing planes defined from external landmarks, and the researchers computed the interobserver reliability ratio of gyral parcellation by comparing the common voxel assignment by 2 observers. They reported 0.64 for SFG, 0.88 for MFG, and 0.92 and 0.88 for 2 separate parts of the IFG. Although this reporting gives a better indication of the agreement of the location of the regions between 2 raters than simply comparing volumes, the reliability was defined through its variance as a percentage of total variance of the volume, thus preventing a direct evaluation of whether the same voxels have been marked with the same labels by different observers. A study conducted by Convit at al[21] evaluated the reproducibility of the parcellation method of computing intraclass correlation coefficients by marking only 1 hemisphere of 5 young individuals (37 $\pm$ 8 years), with no validation applied to the older subjects in the study (70 $\pm$ 5.5 years old). No study to date reports both volume and spatial overlap when a protocol is repeated in either normal subjects or in those with neurodegenerative disease.

In contrast, we validated our tracing method in 2 observers by evaluating intra-rater and inter-rater variability in terms of both VSC and spatial SOC. The subject data used included a combination of healthy elderly control subjects and patients with dementia who had various levels and patterns of tissue loss, which modified the relative location, size, and shape of structures and their defining landmarks. Both VSC and SOC were close to 1 and thus confirmed the reliability and reproducibility of the proposed parcellation method. The agreement between the 2 different raters was very high (0.91, VSC; 0.85, SOC). Our results showed that our proposed parcellation method provided comparable accuracy in control subjects and subjects with 2 common neurodegenerative conditions (Figs 8 and 9), confirming that the definitions used were not biased by the global cortical displacements related to neurodegeneration.

Local topographic features of the frontal cortex defined the regions of interest we segmented; we used sulci with high-continuity rates that are easily identifiable even in the presence of later stage neurodegeneration. On average, the SOCs had slightly lower values than the volume coefficients (Tables 1 and 2). This difference gives us a measure of how consistently the actual anatomic locations were labeled and is therefore a more sensitive measure of the reproducibility of the anatomic definition and its ability to truly localize a volumetric measurement. Overall the SOC for the 2 different raters was slightly higher when using the second tracing of the observer who traced the test set twice (0.85 versus 0.83), which probably indicates a level of learning and improvement with time toward a consistent marking.

The proposed approach in this work differs from preexisting methods in several important aspects:

Feature-Based Borders. We strictly avoided contrived external reference points or imaginary planes. Many previous parcellation methods relied on the definition of reference planes orthogonal to the line through the anterior and the posterior commissures to inscribe various gyral and lobar borders.[7] Although convenient, this approach cannot produce consistent volumes across subjects in whom local and global

atrophy may modify the spatial relationships between the regions of interest and the external landmarks.

Orientation Independence. Our procedure does not require alignment in space across subjects, which itself can introduce bias into the marking process when structural changes have occurred in the brain. The tools used provided free-form interaction with the data that were evaluated, without enforcing a reference orientation, and produced parcellations on the intrinsic voxel grid of the acquired data. Many authors define structural borders by counting sections away from a particular landmark[22] or superimposing grids.[23] These approaches are prone to introducing additional volumetric bias due to changes in the relationship between structures of interest and external reference landmarks.

Degenerated Tissues. Published parcellation methods have generally involved healthy subjects or patients with pathologies that do not severely modify gyral structure, such as schizophrenia and depression.[24] Our subjects were elderly healthy controls and patients with AD and LBD who manifested considerable tissue degeneration.

Conclusion

We described the development and validation of a new parcellation scheme that takes into account cortical variability and changes induced in neurodegeneration.

The quantitative validation of our method, making use not only of volume agreement but also of the spatial overlap between the different parcellations, shows the presented method to be a successful approach to quantitative cortical comparisons: The method is a useful tool for regional parcellation of structural MR imaging volumes in the frontal lobe area. The parcellation approach provides a clearer definition of the areas of damage for comparison with functional findings. Overall the method we used to define regions of interest performed equally well with controls and patients with neurodegenerative pathology. The cortical tissue displacements possible in neurodegenerative disease did not affect our method because no external references were used and all the structures were evaluated in their acquired coordinate frame.

This protocol, along with the software tools used to apply it, is presented as a resource for other investigators. The information from the current protocol can be incorporated into larger systematic evaluations of brain surface, variability, and volume,[25] providing a contribution to the advancement of versatile 3D brain atlases.[26] The high reproducibility of the proposed frontal lobe borders in subjects with LBD, patients with AD, and aged-matched healthy controls makes it a consistent tool that can be used for volumetric evaluation of pathology. Parcellated structural MR imaging can be co-registered with other imaging techniques and can thus aid in the localization of activity changes in functional neuroimaging studies. The regions of interest defined here can be used as a basis for creating automated parcellation algorithms,[27] which replace these labor-intensive manual procedures in comparative studies of dementia.

Acknowledgments

We thank D. Truran, F. Rousseau, C. Rodriguez, and J. Kornak for the helpful discussions and advice.

References

1. Caviness VS Jr, Lange NT, Makris N, et al. **MRI-based brain volumetrics: emergence of a developmental brain science.** *Brain Dev* 1999;21:289–95
2. Hsu YY, Du AT, Schuff N, Wei, et al. **Magnetic resonance imaging and magnetic resonance spectroscopy in dementias.** *J Geriatr Psychiatry Neurol* 2001; 14:145–66
3. Tzourio N, Petit L, Mellet E, et al. **Use of anatomical parcellation to catalog and study structure: function relationships in the human brain.** *Hum Brain Mapp* 1997;5:228–32
4. Wright JC, McGuire PK, Poline JB, et al. **A voxel-based method for the statistical analysis of gray and white matter density applied to schizophrenia.** *Neuroimage* 1995;2:244–52
5. Bookstein FL. **"Voxel-based morphometry" should not be used with imperfectly registered images.** *Neuroimage* 2001;14:1454–62
6. Buchanan RW, Vladar K, Barta PE, et al. **Structural evaluation of the prefrontal cortex in schizophrenia.** *Am J Psychiatry* 1998;155:1049–55
7. Crespo-Facorro B, Kim JJ, Andreasen NC, et al. **Human frontal cortex: an MRI-based parcellation method.** *Neuroimage* 1999;10:500–19
8. Brodmann K. *Vergleichende localisationslehre der grosshirnrinde in ihren principien dargestellt auf grund des zellenbaues.* Leipzig, Germany: Barth; 1909. Garey LJ, trans-ed. *Brodmann's Localisation in the Cerebral Cortex.* London, UK: Smith-Gordon; 1994
9. Tosun D, Rettmann ME, Han X, et al. **Cortical surface segmentation and mapping.** *Neuroimage* 2004;23(suppl 1):S108–18
10. Ono M, Kubik S, Abernathey CD, eds. *Atlas of the Cerebral Sulci.* Stuttgart, Germany: Thieme Medical Publishers; 1990
11. Kennedy DN, Lange N, Makris N, et al. **Gyri of the human neocortex: an MRI-based analysis of volume and variance.** *Cereb Cortex* 1998;8:372–84
12. Crespo-Facorro B, Kim J, Andreasen NC, et al. **Cerebral cortex: a topographic segmentation method using magnetic resonance imaging.** *Psychiatry Res* 2000; 100:97–126
13. Paus T, Tomaiuolo F, Otaky N, et al. **Human cingulate and paracingulate sulci: pattern, variability, asymmetry, and probabilistic map.** *Cereb Cortex* 1996;1: 207–14
14. Yucel M, Stuart GW, Maruff P, et al. **Paracingulate morphologic differences in males with established schizophrenia: a magnetic resonance imaging morphometric study.** *Biol Psychiatry* 2002;52:15–23
15. Duvernoy HM. **The human brain.** In: Cappabianca P, Alfieri A, de Divitiis E, et al., eds. *Atlas of Endoscopic Anatomy for Endonasal Intracranial Surgery.* 2nd ed. New York: Springer-Verlag/Wien; 2001:214–43
16. Tomaiuolo F, MacDonald JD, Caramanos Z, et al. **Morphology, morphometry and probability mapping of the pars opercularis of the inferior frontal gyrus: an in vivo MRI analysis.** *Eur J Neurosci* 1999;11:3033–46
17. Chiavaras MM, LeGoualher G, Evans A, et al. **Three-dimensional probabilistic atlas of the human orbitofrontal sulci in standardized stereotaxic space.** *Neuroimage* 2001;13:479–96
18. Iosifescu DV, Shenton ME, Warfield SK, et al. **An automated registration algorithm for measuring MRI subcortical brain structures.** *Neuroimage* 1997;6: 13–25
19. Dawant BM, Hartmann SL, Thirion JP, et al. **Automatic 3-D segmentation of internal structures of the head in MR images using a combination of similarity and free-form transformations. Part I. Methodology and validation on normal subjects.** *IEEE Trans Med Imaging* 1999;18:909–16
20. Tisserand DJ, Pruessner JC, Sanz Arigita EJ, et al. **Regional frontal cortical volumes decrease differentially in aging: an MRI study to compare volumetric approaches and voxel-based morphometry.** *Neuroimage* 2002;17:657–69
21. Convit A, Wolf OT, de Leon MJ, et al. **Volumetric analysis of the pre-frontal regions: findings in aging and schizophrenia.** *Psychiatry Res* 2001;107:61–73
22. Wible CG, Shenton ME, Fischer IA, et al. **Parcellation of the human prefrontal cortex using MRI.** *Psychiatry Res* 1997;76:29–40
23. Kates WR, Frederikse M, Mostofsky SH, et al. **MRI parcellation of the frontal lobe in boys with attention deficit hyperactivity disorder or Tourette syndrome.** *Psychiatry Res* 2002;116:63–81
24. Ballmaier M, Toga AW, Blanton RE, et al. **Anterior cingulate, gyrus rectus, and orbitofrontal abnormalities in elderly depressed patients: an MRI-based parcellation of the prefrontal cortex.** *Am J Psychiatry* 2004;161:99–108
25. Allen JS, Damasio H, Grabowski TJ. **Normal neuroanatomical variation in the human brain: an MRI-volumetric study.** *Am J Phys Anthropol* 2002;118:341–58
26. Toga AW, Thompson PM. **Maps of the brain.** *Anat Rec* 2001;265:37–53
27. Bokde AL, Teipel SJ, Zebuhr Y, et al. **A new rapid landmark-based regional MRI segmentation method of the brain.** *J Neurol Sci* 2002;194:35–40